AIAA SciTech Forum
23-27 January 2023, National Harbor, MD & Online
AIAA SCITECH 2023 Forum

10.2514/6.2023-2072

Data-Driven Time-Varying Eigensystem Realization Algorithm With Data-Correlation

Damien Guého*[1], Matthew Brownell†[1], and Puneet Singla‡[1]
[1]*The Pennsylvania State University, University Park, PA, 16802*

Different data-driven system identification methods and algorithms in the field of structures have been developed, analyzed, and tested for modal parameter identification but inherent nonlinearities and noise in the data can drastically limit the application of such methods in order to adequately describe the real system behavior. While classical state-space realization techniques are, in essence, a least-squares fit to the pulse response measurements, introducing output auto-correlation and cross-correlations over a defined number of lag values has the potential to temper the effect of noise. This paper introduces a data-correlation approach to the time-varying eigensystem realization algorithm (TVERA/DC). As motivational cases to support this new method, the identification of the vibrational characteristics of a space structure is considered as well as the dynamical identification of a mechanical system with time-varying angular velocity.

I. Introduction

As the requirements of space missions continue to grow in complexity, so do the required geometries of the spacecraft. Large deployable structures on spacecraft have become of increased interest for both scientific measurements and solar energy collection. These structures have large geometries that cannot be treated under rigid-body assumptions. Understanding the vibrational characteristics of these structures is paramount to their mission's success. One concept to measure the structural shape is to distribute sensors over the surface of the spacecraft and utilize this information to obtain a data-driven model. The output at any given time is considered a function of the input signal, which is a function of time. Implicitly, we assume that the input-output data is sufficiently rich and the identified model will be accurate over a wide class of inputs. This model can also be useful for other purposes such as controlling the system.

The recent advances in machine learning, such as artificial neural network (ANN), can be used to find a global continuous map from system input space to system output space; however, the performance of these algorithms decreases drastically as the dimension of the system output vector increases. To make this point more clear, consider

*Graduate Student, Department of Aerospace Engineering, AIAA Student Member, AAS Student Member, djg76@psu.edu.
†Graduate Student, Department of Aerospace Engineering, AIAA Student Member, AAS Student Member, mtb5476@psu.edu.
‡Professor, Department of Aerospace Engineering, AIAA Associate Fellow, AAS Fellow, psingla@psu.edu

a problem of active control of a flexible space structure. Generally, the system output vector consists of surface distortion measurements at various spatial points, $O(10^3)$, which are measured by sensors like strain gauges, suns sensors, stereo vision systems, LIDAR, etc. Therefore, if one seeks a dynamic continuous map between the system output and input vectors then the dimension of such a map can be as large as the number of measurements, i.e., $O(10^3)$. However, the dimension of the hidden states of the true system corresponds to the number of dynamic structural modes of interest. The number of these modes are typically less than 10. So, a system identification algorithm is desired that can approximate the system output well, while keeping the dimension of the dynamic map as low as possible.

Many algorithms have been established, some of them deterministic in nature, i.e. without considering noise in the measured data, and others stochastic, i.e. with formulations minimizing the noise uncertainty in the identification. During the 90s, building upon initial work by Gilbert and Kalman, several methods have been developed to identify the most observable and controllable subspace of the system from given input-output (I/O) data [1–5]. Under the interaction of structure and control disciplines, the eigensystem realization algorithm (ERA) [3, 4] was developed for modal parameter identification and model reduction of dynamic systems using test data. The algorithm presents a unified framework for modal parameter identification based on the Markov parameters (i.e., pulse response) making it possible to construct a Hankel matrix as the basis for the realization of a discrete-time state-space model. A few years later at NASA, Juang developed a method for simultaneously identify a linear state-space model and the associated Kalman filter from noisy input-output measurements. Known as the observer/Kalman identification algorithm (OKID) and formulated entirely in the time-domain, it computes the Markov parameters of a linear system, from which the state-space model and a corresponding observer are determined simultaneously [6, 7]. The method relies on an observer equation to compress the dynamics of the system and efficiently estimate the associated system parameters (Markov parameters). In conjunction with the ERA, the method provides simultaneously both the Markov parameters and the Kalman gain, extracting all the possible information present in the data. The observer at the core of the method was proven to be the steady-state Kalman filter corresponding to the system to be identified. Later, the ERA with data correlation (ERA/DC) is developed [8–11] and while the ERA is, in essence, a least-squares fit to the pulse response measurements, the ERA/DC involves a fit to the output auto-correlation and cross-correlations over a defined number of lag values.

However, the main difficulty in linear system identification applications stems from the interplay of noise and unmodeled dynamics. Noise, finite length of data, and parameters variation are some of the issues that limit the application of such methods and there are many instances when this limitation is significant enough that it becomes necessary to deal with situations where no model in the model set can adequately describe the real system behavior. In addition, most systems are only linear to a first approximation. Depending on the excitation level, the output is disturbed by nonlinear distortions so that the linearity assumption no longer holds. This immediately limits the application of the results obtained

by the linear system identification framework. In parallel, several efforts have been made for developing time-varying models and to generalize ERA to the case of time-varying systems. Development of methods for time-varying systems have involved recursive and fast implementations of the time invariant methods by exploring structural properties of the input–output realizations [12] or by generalizing several concepts in the classical linear time invariant system theory consistently [5, 13]. Later, the idea of repeated experiments have been introduced [14, 15] and presented as practical methods to realize the conceptual state space model identification strategies presented earlier. The literature in linear time varying system identification is limited as compared to LTI system identification by the fact that there are no approaches to find similarity transformations between the model sequences. In our earlier work [16, 17], it is shown that there exist special reference frames, in which the identified models are similar to the true model, i.e., state transition matrices share the same eigenvalues. Using this key result the realizations can be compared across different data sets. This forms the basis for spectral characterization of the time varying systems and the resulting algorithm is known as the time-varying eigensystem realization algorithm (TVERA). This paper exploits the TVERA formulation in conjunction with the important notion of kinematically similar (topologically equivalent) realizations to assess the validity of the resulting identified model. Similarly as for ERA/DC, it is possible to introduce a fit to the output auto-correlation and cross-correlations for TVERA. The bias terms affecting the TVERA when "white" measurement noise is present can be omitted in the TVERA/DC by properly tuning some of the parameters. The computational steps for the TVERA/DC are almost identical

This paper aims to demonstrate the benefits of including data correlations when in presence of noisy measurements. Section II will explain the basic concepts of data-correlation for time-invariant system realization (ERA/DC) and will provide a description of this procedure adapted for time-varying system identification, introducing the time-varying eigensystem realization algorithm with data-correlation (TVERA/DC). To validate this data-correlation approach, Section III will consider two examples where the goal is to reproduce the response of a dynamical system from rogue sensor measurements.

II. Subspace system identification with data-correlation

A discrete-time invariant linear system can be represented by

$$\boldsymbol{x}_{k+1} = A\boldsymbol{x}_k + B\boldsymbol{u}_k \tag{1a}$$

$$\boldsymbol{y}_k = C\boldsymbol{x}_k + D\boldsymbol{u}_k \tag{1b}$$

together with an initial state vector $\boldsymbol{x}_0$, where $\boldsymbol{x}_k \in \mathbb{R}^n$, $\boldsymbol{u}_k \in \mathbb{R}^r$ and $\boldsymbol{y}_k \in \mathbb{R}^m$ are the state, control input and output vectors respectively. The constant matrices $A \in \mathbb{R}^{n\times n}$, $B \in \mathbb{R}^{r\times n}$, $C \in \mathbb{R}^{n\times m}$ and $D \in \mathbb{R}^{r\times m}$ represent the internal operation of the linear system, and are used to determine the system's response to any input.

The basic development of the state-space realization is attributed to Ho and Kalman [2] who introduced the important principles of minimum realization theory. The Ho-Kalman procedure uses the Hankel matrix to construct a state-space representation of a linear system from noise-free data. The methodology has been modified and substantially extended to develop the Eigensystem Realization Algorithm (ERA) [3] to identify modal parameters from measurement data.

A. Time-invariant linear system identification: the eigensystem realization algorithm with data correlation (ERA/DC)

The eigensystem realization algorithm with data correlations (ERA/DC) includes an additional fit to output correlations whereas the ERA is basically a least-square fit to the pulse response measurements only. The bias terms affecting the ERA when noise is present can, in principle, be omitted in the ERA/DC by properly tuning some of the parameters. The computational steps of the ERA/DC are outlined in this section.

1. Block Correlation Hankel Matrices

The ERA method with data correlation requires the definition of a square matrix of order $\gamma = pm$,

$$\boldsymbol{\mathcal{R}}_{\boldsymbol{HH}}(k) = \boldsymbol{H}(k)\boldsymbol{H}(0)^{\top} \tag{2}$$

$$= \begin{bmatrix} h_{k+1} & h_{k+2} & \cdots & h_{k+q} \\ h_{k+2} & h_{k+3} & \cdots & h_{k+q+1} \\ \vdots & \vdots & \ddots & \vdots \\ h_{k+p} & h_{k+p+1} & \cdots & h_{k+p+q-1} \end{bmatrix} \begin{bmatrix} h_1 & h_2 & \cdots & h_q \\ h_2 & h_3 & \cdots & h_{q+1} \\ \vdots & \vdots & \ddots & \vdots \\ h_p & h_{p+1} & \cdots & h_{p+q-1} \end{bmatrix}^{\top} \tag{3}$$

$$= \begin{bmatrix} \sum_{i=1}^{q} h_{k+i}h_i^{\top} & \sum_{i=1}^{q} h_{k+i}h_{i+1}^{\top} & \cdots & \sum_{i=1}^{q} h_{k+i}h_{p+i-1}^{\top} \\ \sum_{i=1}^{q} h_{k+i+1}h_i^{\top} & \sum_{i=1}^{q} h_{k+i+1}h_{i+1}^{\top} & \cdots & \sum_{i=1}^{q} h_{k+i+1}h_{p+i-1}^{\top} \\ \vdots & \vdots & \ddots & \vdots \\ \sum_{i=1}^{q} h_{k+p+i-1}h_i^{\top} & \sum_{i=1}^{q} h_{k+p+i-1}h_{i+1}^{\top} & \cdots & \sum_{i=1}^{q} h_{k+p+i-1}h_{p+i-1}^{\top} \end{bmatrix}. \tag{4}$$

where h_k are Markov parameters in the case of forced systems or directly outputs of the system in the case of autonomous systems. Hankel matrices $\boldsymbol{H}(k)$ are defined the same way as in the ERA. Note that the data correlation matrix $\boldsymbol{\mathcal{R}}_{\boldsymbol{HH}}(k)$ can be smaller in size than the Hankel matrix $\boldsymbol{H}(k)$ if $qr \leq pm = \gamma$. For the case when $k = 0$, the correlation matrix

$\mathcal{R}_{\boldsymbol{HH}}(0)$ becomes

$$\mathcal{R}_{\boldsymbol{HH}}(0) = \boldsymbol{H}(0)\boldsymbol{H}(0)^{\top} \tag{5}$$

$$= \begin{bmatrix} h_1 & h_2 & \cdots & h_q \\ h_2 & h_3 & \cdots & h_{q+1} \\ \vdots & \vdots & \ddots & \vdots \\ h_p & h_{p+1} & \cdots & h_{p+q-1} \end{bmatrix} \begin{bmatrix} h_1 & h_2 & \cdots & h_q \\ h_2 & h_3 & \cdots & h_{q+1} \\ \vdots & \vdots & \ddots & \vdots \\ h_p & h_{p+1} & \cdots & h_{p+q-1} \end{bmatrix}^{\top} \tag{6}$$

$$= \begin{bmatrix} \sum_{i=1}^{q} h_i h_i^{\top} & \sum_{i=1}^{q} h_i h_{i+1}^{\top} & \cdots & \sum_{i=1}^{q} h_i h_{p+i-1}^{\top} \\ \sum_{i=1}^{q} h_{i+1} h_i^{\top} & \sum_{i=1}^{q} h_{i+1} h_{i+1}^{\top} & \cdots & \sum_{i=1}^{q} h_{i+1} h_{p+i-1}^{\top} \\ \vdots & \vdots & \ddots & \vdots \\ \sum_{i=1}^{q} h_{p+i-1} h_i^{\top} & \sum_{i=1}^{q} h_{p+i-1} h_{i+1}^{\top} & \cdots & \sum_{i=1}^{q} h_{p+i-1} h_{p+i-1}^{\top} \end{bmatrix}. \tag{7}$$

The matrix $\mathcal{R}_{\boldsymbol{HH}}(0)$ consists of auto-correlations of Markov parameters such as $\sum_{i=1}^{q} h_i h_i^{\top}$ and cross-correlations such as $\sum_{i=1}^{q} h_i h_{i+1}^{\top}$ at lag time values in the range $\pm p$, summed over q values. If noises in the Markov parameters (or outputs) are not correlated, the correlation matrix $\mathcal{R}_{\boldsymbol{HH}}(0)$ will contain less noise than the Hankel matrix $\boldsymbol{H}(0)$.

In terms of controllability and observability matrices, $\mathcal{R}_{\boldsymbol{HH}}(k)$ can be written as

$$\mathcal{R}_{\boldsymbol{HH}}(k) = \boldsymbol{O}^{(p)} A^k \boldsymbol{R}^{(q)} \boldsymbol{R}^{(q)^{\top}} \boldsymbol{O}^{(p)^{\top}} = \boldsymbol{O}^{(p)} A^k \boldsymbol{R}^{(\gamma)}, \tag{8}$$

where $\boldsymbol{R}^{(\gamma)} = \boldsymbol{R}^{(q)} \boldsymbol{R}^{(q)^{\top}} \boldsymbol{O}^{(p)^{\top}}$.

The data correlation matrix $\boldsymbol{\mathcal{R}_{HH}}(k)$ can be used to form a block correlation Hankel matrix

$$\begin{aligned}\boldsymbol{\mathcal{H}}(k) &= \begin{bmatrix} \boldsymbol{\mathcal{R}_{HH}}(k) & \boldsymbol{\mathcal{R}_{HH}}(k+\tau) & \cdots & \boldsymbol{\mathcal{R}_{HH}}(k+\zeta\tau) \\ \boldsymbol{\mathcal{R}_{HH}}(k+\tau) & \boldsymbol{\mathcal{R}_{HH}}(k+2\tau) & \cdots & \boldsymbol{\mathcal{R}_{HH}}(k+(\zeta+1)\tau) \\ \vdots & \vdots & \ddots & \vdots \\ \boldsymbol{\mathcal{R}_{HH}}(k+\xi\tau) & \boldsymbol{\mathcal{R}_{HH}}(k+(\xi+1)\tau) & \cdots & \boldsymbol{\mathcal{R}_{HH}}(k+(\xi+\zeta)\tau) \end{bmatrix} \\ &= \begin{bmatrix} \boldsymbol{O}^{(p)} \\ \boldsymbol{O}^{(p)}A^{\tau} \\ \vdots \\ \boldsymbol{O}^{(p)}A^{\xi\tau} \end{bmatrix} A^{k} \begin{bmatrix} \boldsymbol{R}^{(\gamma)} & A^{\tau}\boldsymbol{R}^{(\gamma)} & \cdots & A^{\zeta\tau}\boldsymbol{R}^{(\gamma)} \end{bmatrix} \\ &= \boldsymbol{O}^{(\xi)}A^{k}\boldsymbol{R}^{(\zeta)}. \end{aligned} \tag{9}$$

For the case when $k = 0$,

$$\begin{aligned}\boldsymbol{\mathcal{H}}(0) &= \begin{bmatrix} \boldsymbol{\mathcal{R}_{HH}}(0) & \boldsymbol{\mathcal{R}_{HH}}(\tau) & \cdots & \boldsymbol{\mathcal{R}_{HH}}(\zeta\tau) \\ \boldsymbol{\mathcal{R}_{HH}}(\tau) & \boldsymbol{\mathcal{R}_{HH}}(2\tau) & \cdots & \boldsymbol{\mathcal{R}_{HH}}((\zeta+1)\tau) \\ \vdots & \vdots & \ddots & \vdots \\ \boldsymbol{\mathcal{R}_{HH}}(\xi\tau) & \boldsymbol{\mathcal{R}_{HH}}((\xi+1)\tau) & \cdots & \boldsymbol{\mathcal{R}_{HH}}((\xi+\zeta)\tau) \end{bmatrix} \\ &= \begin{bmatrix} \boldsymbol{O}^{(p)} \\ \boldsymbol{O}^{(p)}A^{\tau} \\ \vdots \\ \boldsymbol{O}^{(p)}A^{\xi\tau} \end{bmatrix} \begin{bmatrix} \boldsymbol{R}^{(\gamma)} & A^{\tau}\boldsymbol{R}^{(\gamma)} & \cdots & A^{\zeta\tau}\boldsymbol{R}^{(\gamma)} \end{bmatrix} \\ &= \boldsymbol{O}^{(\xi)}\boldsymbol{R}^{(\zeta)}. \end{aligned} \tag{10}$$

τ is an integer chosen to chosen to prevent significant overlap of adjacent correlation blocks. The matrices $\boldsymbol{R}^{(\zeta)}$ and $\boldsymbol{O}^{(\xi)}$ are called the block correlation controllability and observability matrices.

2. Hankel norm approximation

Similarly to the ERA, the ERA/DC process continues with the factorization of the block correlation matrix $\boldsymbol{\mathcal{H}}(0)$ using singular value decomposition so that

$$\boldsymbol{\mathcal{H}}(0) = \boldsymbol{\mathcal{U}}\boldsymbol{\Sigma}\boldsymbol{\mathcal{V}}^{\top} = \begin{bmatrix} \boldsymbol{\mathcal{U}}^{(n)} & \boldsymbol{\mathcal{U}}^{(0)} \end{bmatrix} \begin{bmatrix} \boldsymbol{\Sigma}^{(n)} & \mathbf{0} \\ \mathbf{0} & \boldsymbol{\Sigma}^{(0)} \end{bmatrix} \begin{bmatrix} \boldsymbol{\mathcal{V}}^{(n)\top} \\ \boldsymbol{\mathcal{V}}^{(0)\top} \end{bmatrix} = \boldsymbol{\mathcal{U}}^{(n)}\boldsymbol{\Sigma}^{(n)}\boldsymbol{\mathcal{V}}^{(n)\top} + \underbrace{\boldsymbol{\mathcal{U}}^{(0)}\boldsymbol{\Sigma}^{(0)}\boldsymbol{\mathcal{V}}^{(0)\top}}_{\simeq \mathbf{0}} \simeq \boldsymbol{\mathcal{U}}^{(n)}\boldsymbol{\Sigma}^{(n)}\boldsymbol{\mathcal{V}}^{(n)\top}, \tag{11}$$

and

$$\boldsymbol{\mathcal{H}}(0) = \boldsymbol{\mathcal{U}}^{(n)}\boldsymbol{\Sigma}^{(n)}\boldsymbol{\mathcal{V}}^{(n)\top} = \boldsymbol{O}^{(\xi)}\boldsymbol{R}^{(\zeta)} \Rightarrow \begin{cases} \boldsymbol{O}^{(\xi)} = \boldsymbol{\mathcal{U}}^{(n)}\boldsymbol{\Sigma}^{(n)\,1/2} \\ \boldsymbol{R}^{(\zeta)} = \boldsymbol{\Sigma}^{(n)\,1/2}\boldsymbol{\mathcal{V}}^{(n)\top} \end{cases}. \tag{12}$$

Again, this choice makes both $\boldsymbol{O}^{(\xi)}$ and $\boldsymbol{R}^{(\zeta)}$ balanced.

3. Minimum Realization

From Eq. (10) we have directly

$$\boldsymbol{O}^{(p)} = \boldsymbol{E}^{(\gamma)\mathsf{T}}\boldsymbol{O}^{(\xi)} = \boldsymbol{E}^{(\gamma)\top}\boldsymbol{\mathcal{U}}^{(n)}\boldsymbol{\Sigma}^{(n)\,1/2}. \tag{13}$$

From Eq. (10), an expression of $\boldsymbol{R}^{(q)}$ can be found

$$\boldsymbol{R}^{(q)} = \boldsymbol{O}^{(p)\,\dagger}\boldsymbol{H}(0) = \left[\boldsymbol{E}^{(\gamma)\top}\boldsymbol{\mathcal{U}}^{(n)}\boldsymbol{\Sigma}^{(n)\,1/2}\right]^{\dagger}\boldsymbol{H}(0), \tag{14}$$

and a realization is shown to be

$$\hat{A} = \boldsymbol{O}^{(\xi)\,\dagger}\boldsymbol{\mathcal{H}}(1)\boldsymbol{R}^{(\zeta)\,\dagger} = \boldsymbol{\Sigma}^{(n)} - 1/2\boldsymbol{\mathcal{U}}^{(n)\top}\boldsymbol{\mathcal{H}}(1)\boldsymbol{\mathcal{V}}^{(n)}\boldsymbol{\Sigma}^{(n)-1/2}, \tag{15a}$$

$$\hat{B} = \boldsymbol{R}^{(q)}\boldsymbol{E}^{(r)} = \left[\boldsymbol{E}^{(\gamma)\top}\boldsymbol{\mathcal{U}}^{(n)}\boldsymbol{\Sigma}^{(n)\,1/2}\right]^{\dagger}\boldsymbol{H}(0)\boldsymbol{E}^{(r)}, \tag{15b}$$

$$\hat{C} = \boldsymbol{E}^{(m)\top}\boldsymbol{O}^{(p)} = \boldsymbol{E}^{(m)\top}\boldsymbol{E}^{(\gamma)\top}\boldsymbol{\mathcal{U}}^{(n)}\boldsymbol{\Sigma}^{(n)\,1/2}, \tag{15c}$$

$$\hat{D} = h_0. \tag{15d}$$

B. Time-varying linear system identification: the time-varying eigensystem realization algorithm with data-correlation (TVERA/DC)

From a perspective of generalizing the classical Ho-Kalman approach with ERA and ERA/DC, this paper develops an extension of the time-varying eigensystem realization algorithm (TVERA) by including data correlations in the process (TVERA/DC). With the assumption that noises in data are not correlated, the resulting procedure takes advantage of the fact that auto-correlation and cross-correlation between outputs will contain less noise than original outputs.

Consider that we obtained $M \times N$ experiments, arranged in M batches of N experiments. Similarly as the TVERA procedure [16, 17], form the initial condition response experiments Hankel matrix

$$\tilde{\boldsymbol{H}}_k^{(p,N),\#j} = \begin{bmatrix} \boldsymbol{y}_k^{\#1,j} & \boldsymbol{y}_k^{\#2,j} & \cdots & \boldsymbol{y}_k^{\#N,j} \\ \boldsymbol{y}_{k+1}^{\#1,j} & \boldsymbol{y}_{k+1}^{\#2,j} & \cdots & \boldsymbol{y}_{k+1}^{\#N,j} \\ \vdots & \vdots & \ddots & \vdots \\ \boldsymbol{y}_{k+p-1}^{\#1,j} & \boldsymbol{y}_{k+p-1}^{\#2,j} & \cdots & \boldsymbol{y}_{k+p-1}^{\#N,j} \end{bmatrix} = \boldsymbol{O}_k^{(p)} \boldsymbol{X}_k^{(N),\#j}, \quad j = 1 \dots M. \tag{16}$$

$\boldsymbol{O}_k^{(p)} \in \mathbb{R}^{pm \times n}$ is the observability matrix at time k and $\boldsymbol{X}_k^{(N),j}$ is the state variable ensemble matrix of batch j at time k, i.e. the state initial condition responses of experiments of batch j at time k. Whereas the standard TVERA method proceeds using $\tilde{\boldsymbol{H}}_k^{(p,N),j}$ to derive state-space matrices A_k and C_k, the TVERA method with data correlations requires the definition of a square matrix $\tilde{\boldsymbol{\mathcal{R}}}_k^{\#j} \in \mathbb{R}^{pm \times pm}$ such that for $j = 1 \dots M$ we have

$$\tilde{\boldsymbol{\mathcal{R}}}_k^{\#j} = \tilde{\boldsymbol{H}}_k^{(p,N),j} \tilde{\boldsymbol{H}}_0^{(p,N),j^\top} \tag{17a}$$

$$= \begin{bmatrix} \boldsymbol{y}_k^{\#1,j} & \boldsymbol{y}_k^{\#2,j} & \cdots & \boldsymbol{y}_k^{\#N,j} \\ \boldsymbol{y}_{k+1}^{\#1,j} & \boldsymbol{y}_{k+1}^{\#2,j} & \cdots & \boldsymbol{y}_{k+1}^{\#N,j} \\ \vdots & \vdots & \ddots & \vdots \\ \boldsymbol{y}_{k+p-1}^{\#1,j} & \boldsymbol{y}_{k+p-1}^{\#2,j} & \cdots & \boldsymbol{y}_{k+p-1}^{\#N,j} \end{bmatrix} \begin{bmatrix} \boldsymbol{y}_0^{\#1,j} & \boldsymbol{y}_0^{\#2,j} & \cdots & \boldsymbol{y}_0^{\#N,j} \\ \boldsymbol{y}_1^{\#1,j} & \boldsymbol{y}_1^{\#2,j} & \cdots & \boldsymbol{y}_1^{\#N,j} \\ \vdots & \vdots & \ddots & \vdots \\ \boldsymbol{y}_{p-1}^{\#1,j} & \boldsymbol{y}_{p-1}^{\#2,j} & \cdots & \boldsymbol{y}_{p-1}^{\#N,j} \end{bmatrix}^\top \tag{17b}$$

$$= \begin{bmatrix} \sum_{i=1}^{N} \boldsymbol{y}_k^{\#i,j} \boldsymbol{y}_0^{\#i,j^\top} & \sum_{i=1}^{N} \boldsymbol{y}_k^{\#i,j} \boldsymbol{y}_1^{\#i,j^\top} & \cdots & \sum_{i=1}^{N} \boldsymbol{y}_k^{\#i,j} \boldsymbol{y}_{p-1}^{\#i,j^\top} \\ \sum_{i=1}^{N} \boldsymbol{y}_{k+1}^{\#i,j} \boldsymbol{y}_0^{\#i,j^\top} & \sum_{i=1}^{N} \boldsymbol{y}_{k+1}^{\#i,j} \boldsymbol{y}_1^{\#i,j^\top} & \cdots & \sum_{i=1}^{N} \boldsymbol{y}_{k+1}^{\#i,j} \boldsymbol{y}_{p-1}^{\#i,j^\top} \\ \vdots & \vdots & \ddots & \vdots \\ \sum_{i=1}^{N} \boldsymbol{y}_{k+p-1}^{\#i,j} \boldsymbol{y}_0^{\#i,j^\top} & \sum_{i=1}^{N} \boldsymbol{y}_{k+p-1}^{\#i,j} \boldsymbol{y}_1^{\#i,j^\top} & \cdots & \sum_{i=1}^{N} \boldsymbol{y}_{k+p-1}^{\#i,j} \boldsymbol{y}_{p-1}^{\#i,j^\top} \end{bmatrix}. \tag{17c}$$

Let a $\xi \times M$ block correlation Hankel matrix be formed as

$$\tilde{\mathcal{H}}_k^{(\xi,M)} = \begin{bmatrix} \tilde{\mathcal{R}}_k^{\#1} & \tilde{\mathcal{R}}_k^{\#2} & \cdots & \tilde{\mathcal{R}}_k^{\#M} \\ \tilde{\mathcal{R}}_{k+\tau}^{\#1} & \tilde{\mathcal{R}}_{k+\tau}^{\#2} & \cdots & \tilde{\mathcal{R}}_{k+\tau}^{\#M} \\ \vdots & \vdots & \ddots & \vdots \\ \tilde{\mathcal{R}}_{k+(\xi-1)\tau}^{\#1} & \tilde{\mathcal{R}}_{k+(\xi-1)\tau}^{\#2} & \cdots & \tilde{\mathcal{R}}_{k+(\xi-1)\tau}^{\#M} \end{bmatrix} = \begin{bmatrix} \boldsymbol{O}_k^{(p)} \\ \boldsymbol{O}_{k+\tau}^{(p)} \\ \vdots \\ \boldsymbol{O}_{k+(\xi-1)\tau}^{(p)} \end{bmatrix} \begin{bmatrix} \tilde{\boldsymbol{X}}_k^{(p),\#1} & \tilde{\boldsymbol{X}}_k^{(p),\#2} & \cdots & \tilde{\boldsymbol{X}}_{k\tau}^{(p),\#M} \end{bmatrix} \tag{18}$$

$$= \boldsymbol{O}_k^{(\xi)} \tilde{\boldsymbol{X}}_k^{(M)} \tag{19}$$

with $\tilde{\boldsymbol{X}}_k^{(p),\#j} = \boldsymbol{X}_k^{(N),\#j} \boldsymbol{X}_0^{(N),\#j\intercal} \boldsymbol{O}_0^{(p)\intercal} \in \mathbb{R}^{n \times pm}$ for $j = 1 \ldots M$. Now, note that

$$\tilde{\boldsymbol{X}}_{k+1}^{(p),\#j} = \boldsymbol{X}_{k+1}^{(N),\#j} \boldsymbol{X}_0^{(N),\#j\intercal} \boldsymbol{O}_0^{(p)\intercal} = A_k \boldsymbol{X}_k^{(N),\#j} \boldsymbol{X}_0^{(N),\#j\intercal} \boldsymbol{O}_0^{(p)\intercal} = A_k \tilde{\boldsymbol{X}}_k^{(p),\#j}, \quad j = 1 \ldots M. \tag{20}$$

The matrix A_k at time k can be derived as

$$\hat{A}_k = \tilde{\boldsymbol{X}}_{k+1}^{(M)} \tilde{\boldsymbol{X}}_k^{(M)\dagger}, \tag{21}$$

and the output matrix C_k as

$$\hat{C}_k = \boldsymbol{O}_k^{(\xi)}[1:m,:]. \tag{22}$$

Next section will present the approximation capabilities of these two algorithms with respect to their original versions where data-correlation is not included.

III. Example 1: Dynamics of a point mass in a rotating tube

A. Model description

As an illustrative example for the TVERA/DC algorithm, let's consider the dynamics of a point mass in a rotating tube governed by a second order differential equation given by

$$\delta\ddot{r}(t) = \left(\dot{\theta}^2(t) - \frac{k}{m}\right) \delta r(t) + u(t) + l\dot{\theta}^2(t) \tag{23}$$

where the new variable $\delta r(t) = r(t) - l$ has been introduced, together with the definition of l, as the free length of the spring (when no force is applied on it, i.e., Hooke's Law applies as $F_s = -k\delta r$). The function $u(t)$ is the radial control

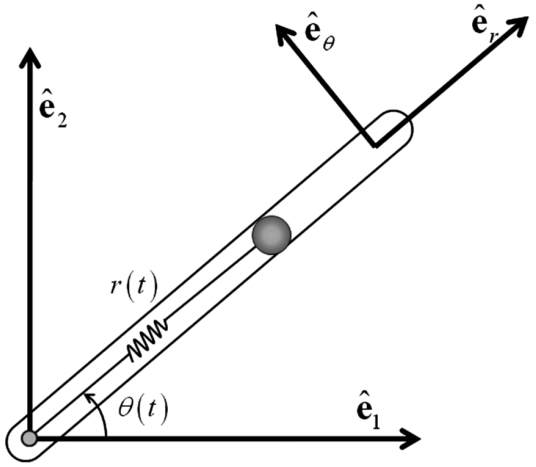

Figure 1 Point mass in a rotating tube setup

force applied on the point mass, and the parameters k and m are the spring stiffness and the mass of the point mass of interest. The time variation in this linear system is brought about by the profile of the angular velocity of the rotating tube $\dot{\theta}(t)$. Choosing the origin of the coordinate system at the position $r_0 = l$ (with no loss of generality), the second order differential equation is given by

$$\delta\ddot{r}(t) = \left(\dot{\theta}^2(t) - \frac{k}{m}\right)\delta r(t) + u(t) \tag{24}$$

where the redefinition of the origin renders the system linear time varying without any extra forcing functions. In the first order state space form ($x_1(t) = \delta r(t), x_2(t) = \delta\dot{r}(t)$), the equations can be written as

$$\begin{bmatrix}\dot{x}_1(t)\\ \dot{x}_2(t)\end{bmatrix} = \begin{bmatrix}0 & 1\\ \dot{\theta}^2(t) - \frac{k}{m} & 0\end{bmatrix}\begin{bmatrix}x_1(t)\\ x_2(t)\end{bmatrix} + \begin{bmatrix}0\\ 1\end{bmatrix}u(t) = A(t)\boldsymbol{x}(t) + B(t)u(t) \tag{25}$$

together with the measurement equations

$$\begin{bmatrix}y_1(t)\\ y_2(t)\end{bmatrix} = \begin{bmatrix}1 & 0\\ 0 & 1\end{bmatrix}\begin{bmatrix}x_1(t)\\ x_2(t)\end{bmatrix} + \begin{bmatrix}0\\ 1\end{bmatrix}u(t) \tag{26}$$

To compare with the identified models, analytical discrete-time models were also generated by computing the state transition matrix (equivalent A_k) and the convolution integrals (equivalent B_k with a zero order hold assumption on the inputs). Because the system matrices are time varying, matrix differential equations are given by

$$\dot{\Phi}(t, t_k) = A(t)\Phi(t, t_k), \qquad \dot{\Psi}(t, t_k) = A(t)\Psi(t, t_k) + I, \tag{27}$$

$\forall\, t \in [t_k, t_{k+1}]$, with initial conditions

$$\Phi(t_k, t_k) = \begin{bmatrix} 1 & 0 \\ 0 & 1 \end{bmatrix}, \quad \Psi(t_k, t_k) = \begin{bmatrix} 0 & 0 \\ 0 & 0 \end{bmatrix} \tag{28}$$

such that

$$A_k = \Phi(t_{k+1}, t_k), \quad B_k = \Psi(t_{k+1}, t_k)B, \tag{29}$$

would represent the equivalent discrete-time varying system (true model). For the current investigation, the time variation profile of $\dot{\theta}(t) = 3\sin(\frac{1}{2}t)$, with the mass and stiffness of the system were chosen to be $m = 1$ and $k = 10$, respectively.

B. Linear time-varying reduced-order model using TVERA/DC

The time interval of interest was held to be 40 seconds, with the discretization sampling frequency set to be 10 Hz. The training is performed on 20 trajectories generated from 20 random initial conditions. A white noise of mean zero and covariance $0.02I_m$ is added to the measurements. Testing of the identified models from both algorithms TVERA and TVERA/DC is performed on 10 random trajectories, not included in the training set. Figure 2 shows the comparison in identification performance. The approximation from TVERA degrades as time increases and while it is able to preserve the frequency content, the amplitude of the identified signal is off after just a few seconds. On the other hand, the signal reconstructed from the TVERA/DC procedure is able to match the true trajectory, up to the noise content. Tables 1 and 2 present the RMS and absolute errors in prediction for models from the two algorithms.

Table 1 RMS Error for 10 trials

TVERA	TVERA/DC
$1.4 \cdot 10^{-1}$	$5.5 \cdot 10^{-2}$

Table 2 Absolute Error for 10 trials

TVERA	TVERA/DC
$1.1 \cdot 10^{-1}$	$4.4 \cdot 10^{-2}$

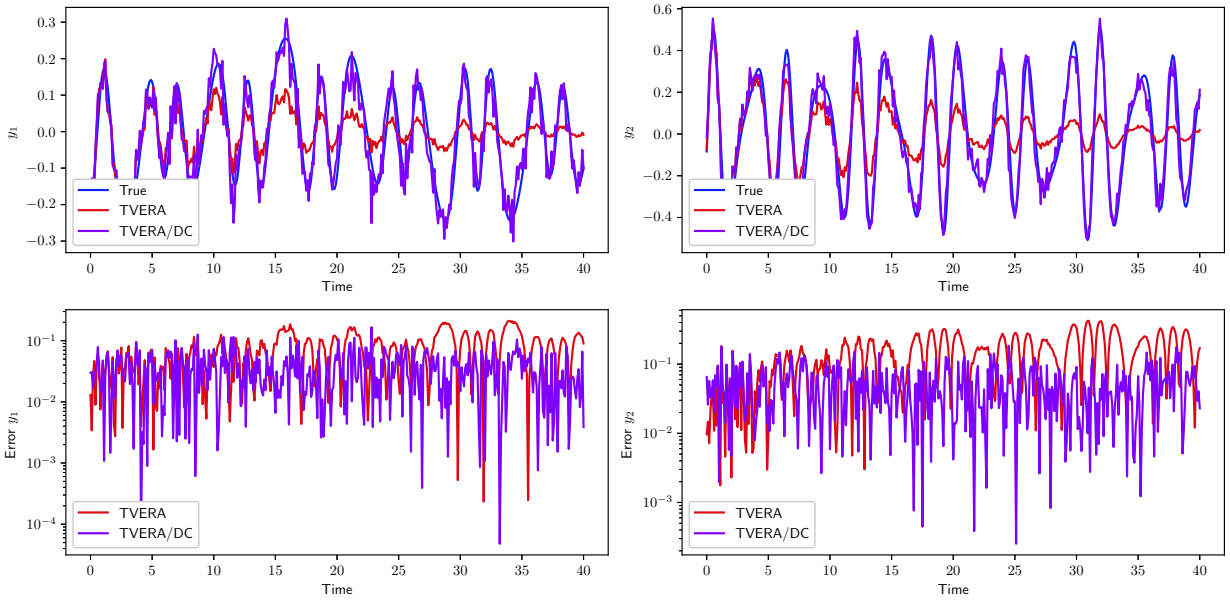

Figure 2 Linear time-varying model identification performance on a testing trajectory

IV. Example 2: Model of a flexible space structure

A. Coupled Rigid and Flexible Body Model

For the purpose of obtaining output data for the various algorithms used in this paper, we consider the vibrations of the spacecraft depicted in Figure 3. This spacecraft is a large, flexible structure whose vibrational modes we wish to study. The structure is modeled as a rigid frame with a flexible membrane clamped within. It is readily apparent that the dynamics of both a rigid and flexible body are well defined; however, this model is simply used as a basis of comparison for the different data-driven algorithms introduced later in this paper. In reality, a similar spacecraft would not have such simple dynamics.

The coupled equations of motion for this model are derived based on the Lagrangian formulation presented in [18], [19] and are omitted from this paper for brevity's sake. Only the resulting equation of motion related to the motion of the membrane is necessary for this analysis. The reference frames and relevant vectors are depicted in Figure 3. The black $\{\hat{\boldsymbol{i}}, \hat{\boldsymbol{j}}, \hat{\boldsymbol{k}}\}$ frame is the inertial-reference frame and the red $\{\hat{\boldsymbol{b}}_1, \hat{\boldsymbol{b}}_2, \hat{\boldsymbol{b}}_3\}$ frame is the body-fixed frame. Now that the basis vectors are defined, we move on to deriving the dynamics of the system.

1. Dynamics

The position vectors shown in Figure 3 are defined as

$$\boldsymbol{r}_{RB} = X\hat{\boldsymbol{b}}_1 + Y\hat{\boldsymbol{b}}_2 + Z\hat{\boldsymbol{b}}_3 \tag{30}$$

$$\boldsymbol{r}_{Flex} = \boldsymbol{r}_{RB} + \boldsymbol{r}_{Mem} \tag{31}$$

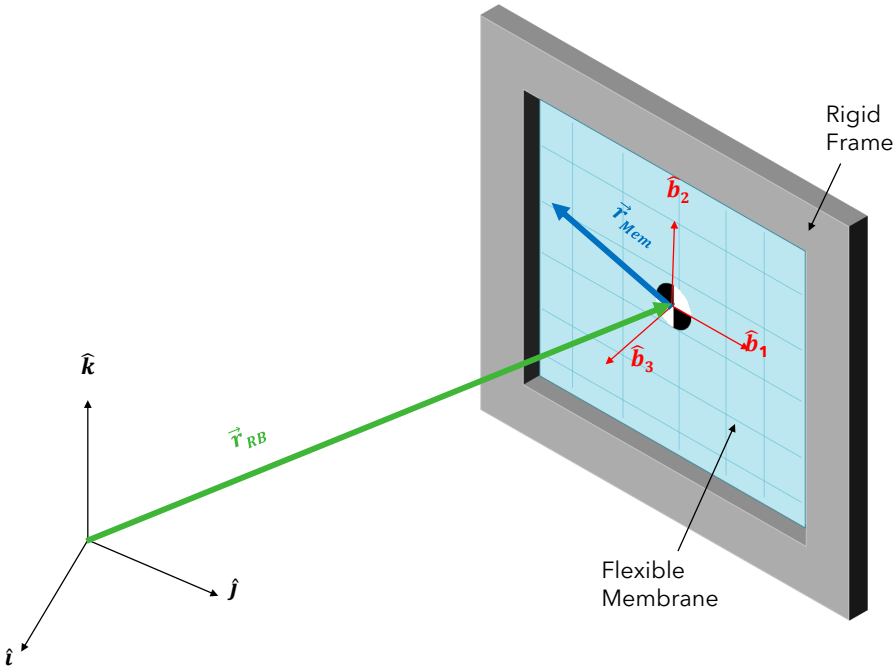

Figure 3 Spacecraft Model and Frame/Vector Definitions

$$\begin{aligned} \boldsymbol{r}_{Flex} &= \boldsymbol{r}_{RB} + x\hat{\boldsymbol{b}}_1 + y\hat{\boldsymbol{b}}_2 + \eta\hat{\boldsymbol{b}}_3 \\ &= (X+x)\hat{\boldsymbol{b}}_1 + (Y+y)\hat{\boldsymbol{b}}_2 + (Z+\eta)\hat{\boldsymbol{b}}_3 \end{aligned} \tag{32}$$

where $\{x, y, \eta\}$ is the position of any membrane element relative to the rigid body's center of mass written in body-fixed coordinates, and $\{X, Y, Z\}$ are the inertial components of the center of mass of the rigid frame also written in body-fixed coordinates.

The full set of differential equations of motion for the spacecraft are omitted from this paper for brevity's sake. For the purposes of this paper, the only necessary equation of motion is

$$\int_{b_1}^{b_2}\int_{a_1}^{a_2} [\rho(\ddot{\boldsymbol{r}}_{Flex}) \cdot \boldsymbol{b}_3 - P\nabla^2\eta]dxdy = \int_{b_1}^{b_2}\int_{a_1}^{a_2} \hat{f}dxdy \tag{33}$$

since our goal is to identify the dynamics of the membrane, not the rigid body dynamics. Note that P is the tension in the membrane, ρ is the two-dimensional density of the membrane, and $\hat{f}$ is an arbitrary distributed load. The integral bounds a_1/a_2 and b_1/b_2 are the x and y bounds of the membrane relative to its geometric center, respectively. Note that we are only considering displacement normal to the membrane's surface, corresponding to the variable η. This meaning there are no transverse vibrations in the $\hat{\boldsymbol{b}}_1$ and $\hat{\boldsymbol{b}}_2$ directions. In the next section, an approach to solving the above partial differential equation is shown.

2. Method of Weighted Residuals

The partial-differential equation shown in equation (33) details the motion of the model's membrane and can be solved numerically by converting it to a system of ordinary differential equations. This is achieved via the Galerkin method of weighted residuals [20]. The displacement of the membrane, $\eta(x, y, t)$, is written as the double sum

$$\eta(x, y, t) = \sum_{i=1}^{n} \sum_{j=1}^{n} \phi_{ij}(x, y) q_{ij}(t) \tag{34}$$

where n^2 is the total number of assumed modes, $\phi_{ij}(x, y)$ are basis functions to be chosen by the user, and $q_{ij}(t)$ are the corresponding modal amplitudes of $\phi_{ij}(x, y)$. The basis functions for $\phi_{ij}(x, y)$ are chosen to be the known basis functions of a fully clamped membrane,

$$\phi_{ij}(x, y) = \sin\left[\frac{i\pi}{a}(x - \frac{a}{2})\right] \sin\left[\frac{j\pi}{b}(y - \frac{b}{2})\right] \qquad i, j = 1, 2, ..., n \tag{35}$$

where a and b are the membrane's width and height, respectively. For the rest of this paper, the double indices will be dropped. Writing in terms of a single index avoids confusion. In the case of $n = 2$, we refer to the modes [(1,1) (1,2) (2,1) (2,2)] instead as modes [1 2 3 4], respectively. This meaning,

$$\phi_i(x, y) := \phi_{jk}(x, y) \qquad \text{where } i = n(j - 1) + k$$

where now $\phi_i(x, y)$ goes from 1 to n^2. For the rest of this paper, n^2 is denoted as N and represents the total number of assumed modes.

Inserting equation (35) into the expanded form of equation (33) leads to,

$$\begin{aligned} \int_{b_1}^{b_2} \int_{a_1}^{a_2} \Big[& \rho \dot{\nu}_3 \phi_j + \rho \phi_i \ddot{q}_i \phi_j + \rho \dot{\omega}_1 y \phi_j - \rho \dot{\omega}_2 x \phi_j - \rho \nu_1 \omega_2 \phi_j + \rho(-\omega_2^2 - \omega_1^2)(\phi_i q_i \phi_j) \\ & + \rho \omega_3 \omega_2 y \phi_j + \rho \omega_1 \nu_2 \phi_j + \rho \omega_1 \omega_3 x \phi_j - P \phi_{x x_i} q_i \phi_j - P \phi_{y y_i} q_i \phi_j - \hat{f} \phi_j \Big] dx dy = 0 \\ & \qquad\qquad i = 1, 2, ..., N \qquad j = 1, 2, ..., N \end{aligned} \tag{36}$$

The derivation of the expression for $\ddot{\boldsymbol{r}}_{Flex}$ is omitted from this paper. In equation (36), $\{\nu_1, \nu_2, \nu_3\}$ are the inertial velocities and $\{\omega_1, \omega_2, \omega_3\}$ are the angular velocities. Both velocities are written in the body-fixed coordinate system.

Note that in equation (36), repeated indices, such as $\phi_i \ddot{q}_i$, represent the full summation of the function we are approximating with our chosen basis functions, whereas ϕ_j represents the basis functions being used as weighting functions in the Galerkin method of weighted residuals. As a result of this, we now have a system of N ordinary differential equations instead of one partial differential equation. The system of equations defined in (36) can be

rearranged into the following form:

$$M\ddot{\boldsymbol{q}} + K\boldsymbol{q} = F \tag{37}$$

where $\boldsymbol{q} \in \mathbb{R}^{N\times 1}$ is a vector of the modal amplitudes. M, K, and F are defined as

$$M_{ij} = \int_{b_1}^{b_2}\int_{a_1}^{a_2}\left[\rho\phi_i\phi_j\right]dxdy \tag{38}$$

$$K_{ij} = \int_{b_1}^{b_2}\int_{a_1}^{a_2}\left[-\rho(\omega_1^2+\omega_2^2)\phi_j - P(\phi_{xx_i}+\phi_{yy_i})\phi_j\right]dxdy \tag{39}$$

$$F_j = \int_{b_1}^{b_2}\int_{a_1}^{a_2}\left[\hat{f} + \rho(-\dot{\nu}_3 - \dot{\omega}_1 y + \dot{\omega}_2 x + \nu_1\omega_2 - \omega_3\omega_2 y - \omega_1\nu_2 - \omega_1\omega_3 x)\right]\phi_j dxdy \tag{40}$$

where $M \in \mathbb{R}^{N\times N}$, $K \in \mathbb{R}^{N\times N}$, and $F \in \mathbb{R}^{N\times 1}$. Here, i and j represent the (i^{th}, j^{th}) element of each matrix and both go from 1 to N. Note that there is no repeated index here so there is no summation in these definitions. In the next section, we will utilize the mass-spring form of equation (37) to obtain a state-space model for our system.

3. State Space Model

By assuming free vibrations ($F_j = 0$), equation (37) can be written as a first-order, continuous, time-varying, linear system of the form:

$$\dot{\boldsymbol{x}} = A_c(t)\boldsymbol{x} \tag{41}$$

$$\boldsymbol{y} = C\boldsymbol{x} \tag{42}$$

where $\boldsymbol{x} \in \mathbb{R}^{2N\times 1}$ is the state vector of time-varying modal amplitudes and their time derivatives and $\boldsymbol{y} \in \mathbb{R}^{m\times 1}$ is the acceleration output vector. The system matrices are written as,

$$A_c = \begin{bmatrix} O^{N\times N} & I^{N\times N} \\ -M^{-1}K(t) & O^{N\times N} \end{bmatrix} \tag{43}$$

$$C = \begin{bmatrix} -C_1M^{-1}K(t) & 0^{mxN} \end{bmatrix} \quad , \quad C_1 = \begin{bmatrix} \phi_1(x_1,y_1) & \dots & \phi_N(x_1,y_1) \\ \vdots & \ddots & \vdots \\ \phi_1(x_m,y_m) & \dots & \phi_N(x_m,y_m) \end{bmatrix} \tag{44}$$

where I and O are the identity and zero matrices, respectively. M and K are the mass and stiffness matrices defined in equations (38) and (39), respectively. Note that the only time-varying aspect of the system comes from the $\omega_1^2 + \omega_2^2$ term

in K (assuming membrane parameters are constant). The output for this system is the acceleration of the membrane at m locations; representing m sensors distributed across the membrane. This is visualized in Figure 4 with a top-down view of the membrane. The black dashed line represents the border of the membrane, the black circle the geometric center, and the red dots the accelerometers.

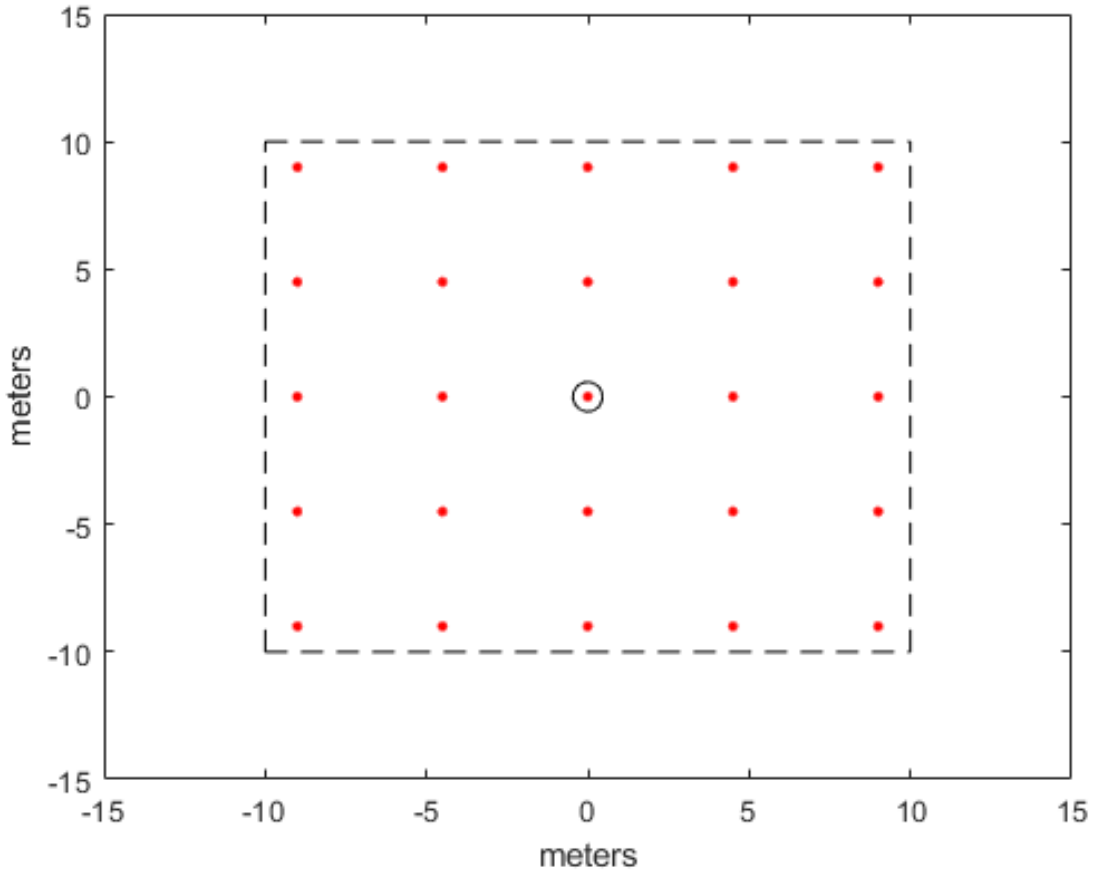

Figure 4 Example of Sensor Placement

For the results in this paper, the first four functions of $\phi_{ij}(x, y)$, defined in equation (35), were chosen as the basis functions (i.e. $i = j = 2$). This implies $A_c \in \mathbb{R}^{8\times 8}$. We can then discretize equations Eq. (41) and Eq. (42) as

$$\boldsymbol{x}_{k+1} = A_k \boldsymbol{x}_k \tag{45}$$

$$\boldsymbol{y}_k = C_k \boldsymbol{x}_k \tag{46}$$

where A_k is the state-transition matrix between time steps, $\Phi(k+1, k)$, and $C_k = C$. We now have our reference discrete state-space model we wish to identify via data-driven modeling. Now, we must utilize this model to obtain output data.

4. Initial Conditions

In order to correctly identify all the dynamics of our derived model, we need to ensure that all modes are excited in our output data. To do this, we choose the initial conditions of our state to be linear combinations of all four assumed flexible body modes, which are the columns of the eigenvector matrix $\Phi = \left[\boldsymbol{\phi}_1, \boldsymbol{\phi}_2, \ldots, \boldsymbol{\phi}_i, \ldots, \boldsymbol{\phi}_{2N}\right]$ obtained from the characteristic equation $|A - \lambda_i| \, \phi_i$. The initial conditions are chosen to be

$$\boldsymbol{x}_{0_i} = r_1(\boldsymbol{\phi}_1 + \boldsymbol{\phi}_2) + r_2(\boldsymbol{\phi}_3 + \boldsymbol{\phi}_4) + r_3(\boldsymbol{\phi}_5 + \boldsymbol{\phi}_6) + r_4(\boldsymbol{\phi}_7 + \boldsymbol{\phi}_8) \quad i = 1, 2, \ldots, K \tag{47}$$

where r_1 through r_4 are random scalars drawn from a normal distribution and K is chosen by the user to ensure enough output data is obtained to capture the order of the system. In the absence of a real input, the initial conditions act as a sort of input instead.

B. Data acquisition and setup description

To obtain the output data for the system, the continuous state-space model defined in Section IV.A.3 was numerically integrated with MATLAB's ode45 function with the initial conditions defined in Section IV.A.4. The following table details the parameter values used in simulation. Note that the two different values of ω_1/ω_2 correspond to two separate cases of a time-invariant and time-varying system. All other parameters remain the same across the two.

N	a	b	ρ	P	ω_1/ω_2	ω_1/ω_2
4	20 m	20 m	5 $\frac{kg}{m^2}$	200 N	0.5 $\frac{rad}{s}$	0.1sin(t) + 0.3 $\frac{rad}{s}$

As for the sensor error, the noise was chosen to have a normal distribution with a standard deviation equal to 5% of the max acceleration the true-system experienced (different for each initial condition case). The different levels of noise will be used for comparison of the different algorithms.

C. Linear time-invariant reduced-order model using ERA/DC

First, linear models are derived from data using the algorithms outlined in the previous section. A hundred random trajectories are considered for the identification, with testing performed on an additional set of 20 trajectories, different from training. Figure 5 shows the performance of the two algorithms on those testing trajectories (average on the 20 trajectories of the testing set). The noise level is indicated as a reference and serves as a lower bound for the identification error. By carefully selecting identification parameters, the eigensystem realization algorithm with data-correlation (ERA/DC) performs up to one order of magnitude better than its ERA counterpart. While non-linearities and noise (rogue sensor measurements here) degrade the approximation capabilities of the ERA, the ERA/DC is less sensitive to noise in the data thanks to correlation calculations. While the relative error induced by the identified model from ERA grows over time and is impacted by measurement noise, the identified model from ERA/DC yields significantly less

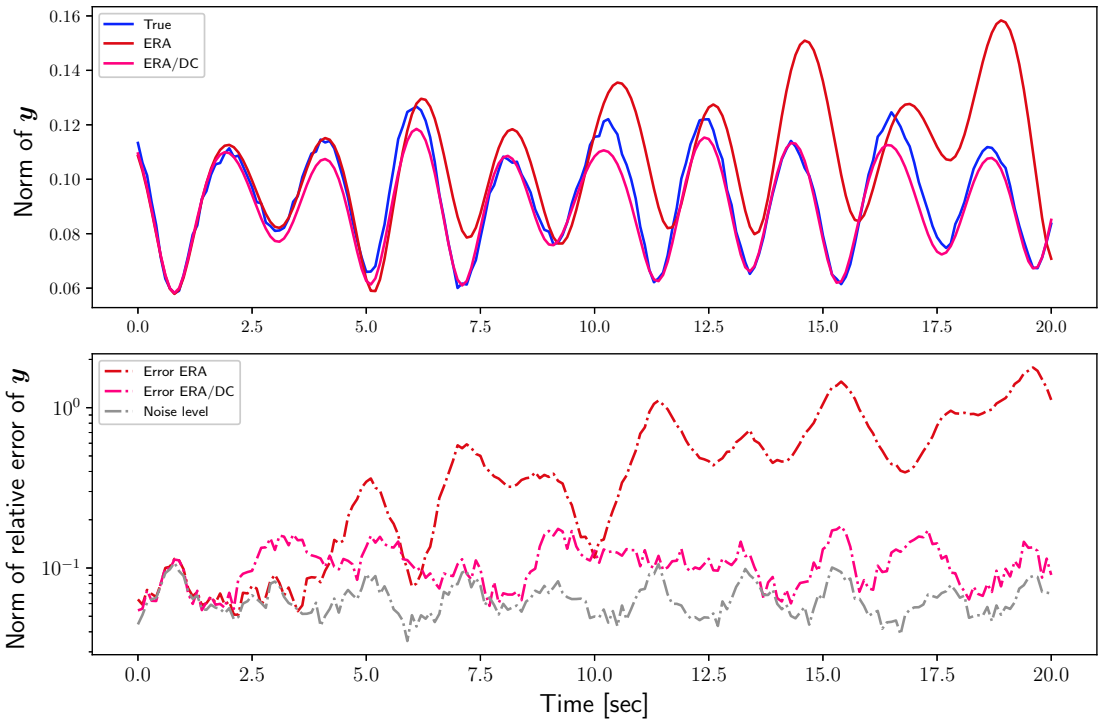

Figure 5 Average linear time-invariant models identification performances on 20 testing trajectories

approximation error and sometimes correctly approximates the response down to - a;most - the non-compressible noise level. The average relative error for the 20 test trials for ERA is at $1.1 \cdot 10^{0}$ while the error from ERA/DC is $7.4 \cdot 10^{-2}$, using the same data set. Models for different of parameter τ have been generated and average errors for the 20 test trajectories are presented in Table 3. This confirms that the bias terms affecting the ERA when measurement noise is present can, in principle, be omitted in the ERA/DC by properly choosing the integer τ.

Table 3 Average relative error for the 20 test trials

Value of parameter τ	Error in approximation from ERA/DC
$\tau = 1$	$1.3 \cdot 10^{0}$
$\tau = 2$	$9.8 \cdot 10^{-1}$
$\tau = 3$	$8.1 \cdot 10^{-1}$
$\tau = 4$	$5.8 \cdot 10^{-1}$
$\tau = 5$	$2.5 \cdot 10^{-1}$
$\tau = 6$	$9.3 \cdot 10^{-2}$
$\tau = 7$	$7.4 \cdot 10^{-2}$

As mentioned earlier, the main difficulty in linear system identification applications stems from the interplay of noise and unmodeled dynamics and most systems are only linear to a first approximation. Since this immediately limits the application of the results obtained by linear system identification algorithms, the time-varying Eigensystem Realization Algorithm with data-correlation is applied to the same data set. Figure 6 shows the performance of the TVERA/DC algorithm to reproduce the system response in presence of noise, where the relative identification error is up to the noise level.

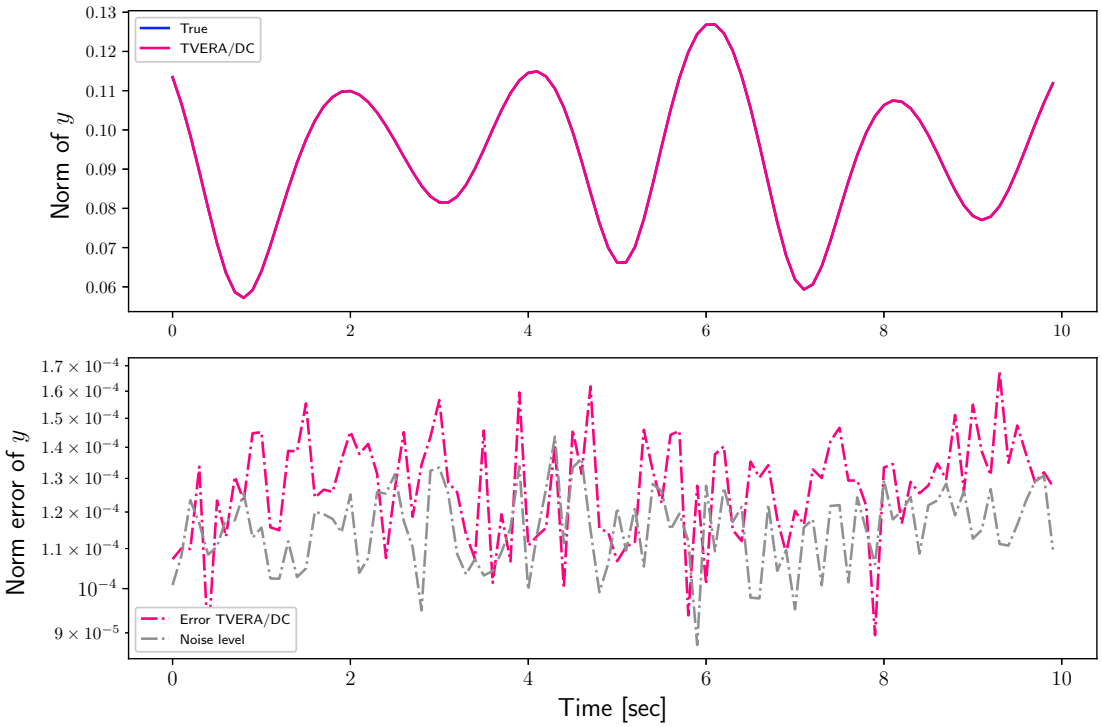

Figure 6 Average linear time-varying models identification performances on 20 testing trajectories

V. Conclusion

Based on a time-invariant state-space realization method, this paper has introduced a data-correlation approach to the time-varying eigensystem realization algorithm (TVERA/DC). It involves a fit to the output auto-correlation and cross-correlations over a defined number of lag values and allows one to temper the effect of noise in the data. Both time-invariant and time-varying versions have been proven successful to reproduce the response of dynamical systems from rogue sensor measurements. The first example shows that noise can affect a basic time-varying identification procedure (TVERA) and can be corrected using TVERA/DC. The second example, of higher dimension, shows that both time-invariant and time-varying models can benefit from data correlation.

References

[1] Gilbert, E. G., "Controllability and Observability in Multivariable Control Systems," *Journal of the Society for Industrial and Applied Mathematics, Series A Control*, Vol. 1, No. 2, 1963, pp. 128–151. doi:https://doi.org/10.1137/0301009.

[2] Ho, B. L., and Kálmán, R. E., "Effective construction of linear state-variable models from input/output functions," *Regelungstechnik*, Vol. 14, No. 12, 1966, pp. 545–548. doi:https://doi.org/10.1524/auto.1966.14.112.545.

[3] Juang, J.-N., and Pappa, R. S., "An Eigensystem Realization Algorithm (ERA) for Modal Parameter Identification and Model Reduction," *Journal of Guidance, Control, and Dynamics*, Vol. 8, No. 5, 1985, pp. 620–627. doi:https://doi.org/10.2514/3.20031.

[4] Juang, J.-N., and Pappa, R. S., "Effects of noise on modal parameters identified by the Eigensystem Realization Algorithm," *Journal of Guidance, Control, and Dynamics*, Vol. 9, No. 3, 1986, pp. 294–303. doi:https://doi.org/10.2514/3.20106.

[5] Shokoohi, S., and Silverman, L. M., "Identification and Model Reduction of Time-varying Discrete-time Systems," *Automatica*, Vol. 23, No. 4, 1987, pp. 509–521.

[6] Juang, J.-N., Phan, M., Horta, L. G., and Longman, R. W., "Identification of Observer/Kalman Filter Markov Parameters: Theory and Experiments," *Journal of Guidance, Control, and Dynamics*, Vol. 16, No. 2, 1993, pp. 320–329. doi:https://doi.org/10.2514/3.21006.

[7] Juang, J.-N., Horta, L. G., Belvin, W. K., Sharkey, J., and Bauer, F. H., "An application of the Observer/Kalman Filter Identification (OKID) technique to Hubble flight data," 1993.

[8] Juang, J.-N., Cooper, J. E., and Wright, J. R., "An Eigensystem Realization Algorithm Using Data Correlation (ERA/DC) for Modal Parameter Identification," *Control Theory and Advanced Technology*, Vol. 4, No. 1, 1988, pp. 5–14.

[9] Anderson, B. D. O., and Skelton, R. E., "The Generation of all q-Markov Covers," *IEEE Transactions on Circuits and Systems*, Vol. 46, 1988, pp. 351–356. doi:https://doi.org/10.1016/S1474-6670(17)55525-1.

[10] Liu, K., Skelton, R. E., and Sharkey, J. P., "Modeling Hubble Space Telescope flight data by Q-Markov cover identification," *Journal of Guidance, Control, and Dynamics*, Vol. 17, No. 2, 1994, pp. 250–256. doi:https://doi.org/10.23919/ACC.1992.4792462.

[11] Skelton, R. E., and Shi, G., "Iterative identification and control using a weighted q-Markov cover with measurement noise," *Signal Processing*, Vol. 52, No. 2, 1996, pp. 217–234. doi:https://doi.org/10.1016/0165-1684(96)00055-2.

[12] Cho, Y. M., Xu, G., and Kailath, T., "Fast Recursive Identification of State Space Models via Exploitation of Displacement Structure," *Automatica*, Vol. 30, No. 1, 1994, pp. 45–59.

[13] Dewilde, P., and Van Der Veen, A. J., *Time Varying Systems and Computations*, Kluwer Academic Publisher, 1998.

[14] Verhaegen, M., *Identification of Time-Varying State Space Models from Input-Output Data*, Workshop on Advanced Algorithms and their Realization, Bonas, 1991.

[15] Verhaegen, M., and Yu, X., "A Class of Subspace Model Identification Algorithms to Identify Periodically and Arbitrarily Time Varying Systems," *Automatica*, Vol. 31, No. 2, 1995, pp. 201–216. doi:https://doi.org/10.1016/0005-1098(94)00091-V.

[16] Majji, M., Juang, J.-N., and Junkins, J. L., "Time-Varying Eigensystem Realization Algorithm," *Journal of Guidance, Control, and Dynamics*, Vol. 33, No. 1, 2010, pp. 13–28. doi:https://doi.org/10.2514/1.45722.

[17] Majji, M., Juang, J.-N., and Junkins, J. L., "Observer/Kalman-Filter Time-Varying System Identification," *Journal of Guidance, Control, and Dynamics*, Vol. 33, No. 3, 2010, pp. 887–900. doi:https://doi.org/10.2514/1.45768.

[18] Junkins, J., and Kim, Y., *Introduction to Dynamics and Control of Flexible Structures*, American Institute of Aeronautics and Astronautics, Inc., 1993.

[19] Dym, C., and Shames, I., *Solid Mechanics: A Variational Approach*, McGraw-Hill Book Company, 1973.

[20] Petrolito, J., "Approximate Solutions of Differential Equations Using Galerkin's Method and Weighted Residuals," *Journal of Mechanical Engineering Education*, Vol. 28, No. 1, 2000, pp. 14–26.